Climate
of the Past

Predicting trends in atmospheric CO$_2$ across the Mid-Pleistocene Transition using existing climate archives

Jordan R. W. Martin[1]**, Joel B. Pedro**[2,3]**, and Tessa R. Vance**[3]

[1]Institute for Marine and Antarctic Studies, University of Tasmania, Hobart, 7004, Australia
[2]Australian Antarctic Division, Kingston, 7050, Australia
[3]Australian Antarctic Program Partnership, Institute for Marine and Antarctic Studies,
University of Tasmania, Hobart, 7004, Australia

Correspondence: Jordan R. W. Martin (jrmartin@utas.edu.au)

Abstract. During the Mid-Pleistocene Transition (MPT), ca. 1200–800 000 years ago (ka), the Earth's glacial cycles changed from 41 to 100 kyr periodicity. The emergence of this longer ice age periodicity was accompanied by higher global ice volume in glacial periods and lower global ice volume in interglacial periods. Since there is no known change in external orbital forcing across the MPT, it is generally agreed that the cause of this transition is internal to the Earth system. Resolving the climate, carbon cycle, and cryosphere processes responsible for the MPT remains a major challenge in Earth and palaeoclimate science. To address this challenge, the international ice core community has prioritised recovery of an ice core record spanning the MPT interval.

Here we present results from a simple generalised least-squares (GLS) model that predicts atmospheric CO$_2$ out to 1.8 Myr. Our prediction utilises existing records of atmospheric carbon dioxide (CO$_2$) from Antarctic ice cores spanning the past 800 kyr along with the existing LR04 benthic $\delta^{18}O_{calcite}$ stack (Lisiecki and Raymo, 2005; hereafter "benthic $\delta^{18}O$ stack") from marine sediment cores. Our predictions assume that the relationship between CO$_2$ and benthic $\delta^{18}O$ over the past 800 000 years can be extended over the last 1.5 million years. The implicit null hypothesis is that there has been no fundamental change in feedbacks between atmospheric CO$_2$ and the climate parameters represented by benthic $\delta^{18}O$, global ice volume, and ocean temperature.

We test the GLS-model-predicted CO$_2$ concentrations against observed blue ice CO$_2$ concentrations, δ^{11}B-based CO$_2$ reconstructions from marine sediment cores, and δ^{13}C of leaf-wax-based CO$_2$ reconstructions (Higgins et al., 2015; Yan et al., 2019; Yamamoto et al., 2022). We show that there is no clear evidence from the existing blue ice or proxy CO$_2$ data to reject our predictions or our associated null hypothesis. A definitive test and/or rejection of the null hypothesis may be provided following recovery and analysis of continuous oldest ice core records from Antarctica, which are still several years away. The record presented here should provide a useful comparison for the oldest ice core records and an opportunity for further constraints on the processes involved in the MPT.

1 Introduction

Ice core records from Antarctica provide comprehensive and continuous records of many climate parameters over the last 800 000 years, e.g. the ice cores from Vostok (Petit et al., 1999) and the European Project for Ice Coring in Antarctica's Dome-C (EDC) (Jouzel et al., 2007). One of the major challenges in climate science lies beyond the current threshold of the ice core record. The Mid-Pleistocene Transition (MPT) spans from ca. 1200–800 000 years ago (ka) (Chalk et al., 2017) and is characterised by a change from regularly paced 40 000-year (kyr) glacial cycles with thinner glacial ice sheets to quasi-periodic 100 kyr glacial cycles in which ice sheets are more persistent and thicker (Clark et al., 2006; Chalk et al., 2017). To resolve the forcings and feedbacks

involved in this transition, multiple nations are targeting recovery of continuous ice cores spanning the MPT under the framework of the International Partnerships in Ice Core Science (IPICS) oldest ice core challenge (IPICS, 2020).

The purpose of the current study is to make a simple prediction of atmospheric CO$_2$ across the MPT. Cross-comparison of our and other predicted CO$_2$ records against observed MPT CO$_2$ data will aid in testing competing hypotheses on the cause of the transition, in particular the role of carbon cycle changes.

The MPT occurred in the absence of any changes to orbital insolation forcing; therefore, the mechanisms behind the MPT must be internal to the Earth system (Raymo, 1997; Ruddiman et al., 1989). Multiple hypotheses have been put forward to explain the transition. A common element in many of these is internal climate–Earth system changes which allow for the development of thicker, more extensive ice sheets that could endure insolation peaks corresponding to the 23 kyr precession and 41 kyr obliquity cycles, i.e. an increase in the threshold for deglaciation and altered sensitivity to orbital forcings (McClymont et al., 2013; Tzedakis et al., 2017). Indeed, the skipped obliquity cycle hypothesis proposes that the 100 kyr signal seen in spectral analysis of the post-MPT benthic δ^{18}O stack (e.g. Fig. 1a) may be comprised of alternating 80 and 120 kyr signals, i.e. in which the intervening obliquity cycles are skipped. Among the prominent hypotheses to explain an increased threshold for deglaciation are the following three.

1. *Long-term decrease in radiative forcing due to a secular reduction in atmospheric CO$_2$ across the transition* (e.g. Berger et al., 1999; Hönisch et al., 2009; Raymo et al., 1988). According to this view, reduced radiative forcing drives the formation of larger and more stable ice sheets.

2. *Progressive removal of sub-glacial regolith during the 41 kyr glacial cycles*. Clark and Pollard (1998) proposed that ice sheet basal sliding prior to the MPT was enhanced by the presence of a low-friction sedimentary regolith layer between the Laurentide ice sheet and the crystalline bedrock. According to this view, progressive removal of this sedimentary layer then favoured the development of larger and more persistent post-MPT ice sheets.

3. *Phase locking of the Northern and Southern Hemisphere ice sheets*. In frequency spectra of the global marine benthic δ^{18}O record (Fig. 1) there is no evidence of the precession (23 kyr) component of Northern Hemisphere insolation prior to the MPT; the spectra are dominated by the obliquity (41 kyr) component (Fig. 1c). Emergence of significant precession and 100 kyr signals occurs across the MPT (Fig. 1b), and all three components are clearly present after the MPT (Fig. 1a). Raymo et al. (2006) suggested that precession-paced changes in Northern and Southern Hemisphere ice volumes may

have occurred prior to the MPT but are cancelled due to out-of-phase ice volume changes between the two hemispheres. According to this view, during the MPT the precession-paced changes fall into phase between the two hemispheres such that the precession signal emerges (Raymo et al., 2006). In this view the global synchronisation of ice volume drives the formation of larger and more stable ice sheets.

These hypotheses are not mutually exclusive. For a recent review on the cause of the MPT see Berends et al. (2021b).

For a long-term decrease in radiative forcing by atmospheric CO$_2$ to be the cause of the MPT, the reduction in CO$_2$ might be expected in both glacial and interglacial stages (Chalk et al., 2017). However, low-resolution boron-isotope-based CO$_2$ reconstructions by Hönisch et al. (2009) and Chalk et al. (2017) suggest that glacial-stage CO$_2$ drawdown occurred over the MPT in the absence of interglacial CO$_2$ drawdown. Glacial-stage CO$_2$ drawdown across the MPT may be a positive climate–carbon cycle feedback to changes in ice sheet dynamics, including CO$_2$ drawdown by enhanced iron fertilisation of the Southern Ocean in response to exposed continental shelves due to lower sea level, as well as planetary drying associated with colder climate conditions (Chalk et al., 2017). Colder glacial temperatures that enhance the solubility of CO$_2$ in the oceans and reduced abyssal ocean ventilation have also been implicated in enhanced glacial-stage ocean storage of CO$_2$ (McClymont et al., 2013; Hasenfratz et al., 2019).

Testing of hypotheses on the cause of the MPT is currently limited by the lack of a continuous ice core that spans its duration. The International Partnership in Ice Core Sciences (IPICS) has nominated recovery of such a record as a key priority in ice core research (IPICS, 2020). Multiple national and international projects have commenced, or are soon to commence, drilling for "oldest ice" (see e.g. Shugi, 2022). In this project, we take inspiration from the "EPICA challenge" in which the palaeoclimate and modelling community was challenged to predict the global atmospheric carbon dioxide and methane concentrations from 800–400 ka based on the existing 400 kyr Vostok ice core record (Wolff et al., 2004). Here, we use a generalised least-squares (GLS) model trained on continuous climate archives to predict a CO$_2$ record out to 1.8 Ma. We utilise two primary datasets for the GLS model: the existing 800 kyr ice core composite record of atmospheric CO$_2$ (Bereiter et al., 2015) and the LR04 benthic stack of 57 globally distributed records of the ^{18}O to ^{16}O ratio of fossil benthic foraminifera calcite (hereafter referred to as the LR04 δ^{18}O benthic stack). The δ^{18}O ratios in the LR04 benthic stack are governed primarily by deep-ocean temperature and global ice volume at the time the foraminifera lived, with higher values indicating both increased ice volume and a colder climate. The relationship between the ice volume and ocean temperature components contributing to the δ^{18}O benthic stack is not linear. Sepa-
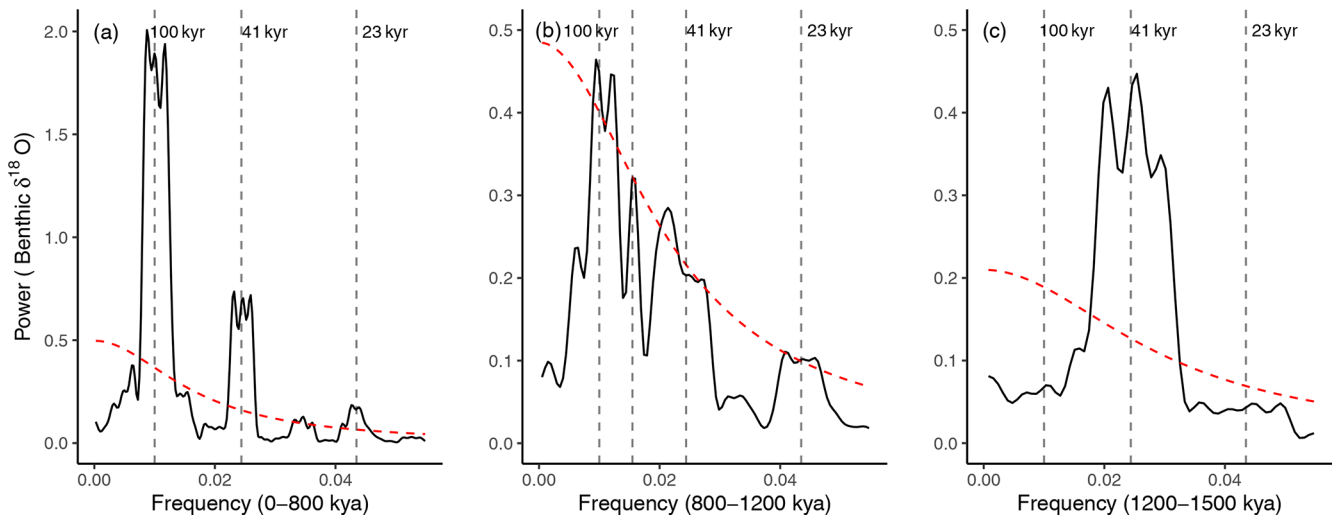
Figure 1. Thomson multi-taper method (MTM) spectral analysis representing the relative power of signal periodicity for **(a)** the benthic δ^{18}O stack after (0–800 ka) the Mid–Pleistocene Transition (MPT), **(b)** benthic δ^{18}O across the MPT (800–1200 ka), and **(c)** benthic δ^{18}O prior to the onset of the MPT (1200–1500 ka). Each has a robust AR(1) 95 % confidence interval (dashed red line). Benthic δ^{18}O stack data are from Lisiecki and Raymo (2005).

rating the two signals remains challenging and has been attempted elsewhere using a range of approaches from comparison with paired deep-ocean temperature proxies (Elderfield et al., 2012) and inverse modelling (Berends et al., 2021a) to spectral analysis (e.g. Huybers and Wunsch, 2005).

Figure 2 shows a scatterplot of the LR04 δ^{18}O benthic stack versus observed ice core CO_2 over the past 800 kyr. Both datasets are binned to equivalent 3 kyr time steps (Methods). The Pearson's correlation coefficient (r) between the datasets is -0.82 ($p < 0.05$), indicating that ~ 68 % of the variance in observed CO_2 is shared with the LR04 δ^{18}O benthic stack. This strong relationship provides an initial rationale for using the LR04 δ^{18}O benthic stack as an input parameter to predict CO_2 beyond 800 kyr. Mechanistically, multiple processes are expected to contribute to the shared variance. A first-order factor is the dependency of CO_2 solubility on ocean temperature (e.g. Millero, 1995). From the simple solubility perspective, colder climate states with increased ice volume and colder ocean temperatures will drive increased ocean uptake of CO_2 (Berends et al., 2021b). However, the solubility effect only accounts for a portion of observed glacial CO_2 drawdown (Archer et al., 2000). Multiple additional contributors to the shared variance are proposed in the literature. These include (not exhaustively) direct radiative forcing of ice volume changes by CO_2 (e.g. Shackleton and Pisias, 1985), the impact of ice volume and/or sea level changes on atmospheric CO_2 via ocean productivity and carbonate chemistry changes (e.g. Broecker, 1982; Archer et al., 2000; Ushie and Matsumoto, 2012), CO_2 drawdown during periods of high ice volume by increased iron fertilisation (e.g. Röthlisberger et al., 2004; Martinez-Garcia et al., 2014), and enhanced sea ice extent during periods of high ice vol-
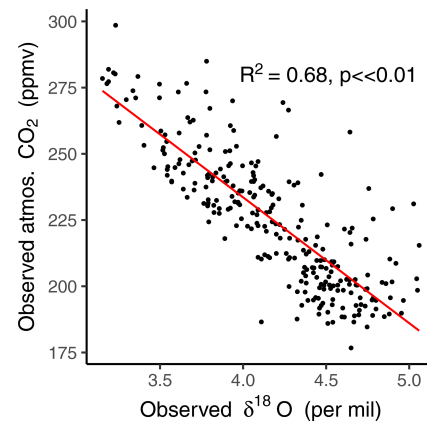
Figure 2. Scatterplot of the composite observed atmospheric CO_2 record (Bereiter et al., 2015) against the LR04 benthic stack of marine δ^{18}O records (Lisiecki and Raymo, 2005). The red line is a linear line of best fit ($R^2 = 0.68$; $p < 0.05$).

ume capping the ventilation of CO_2 from the ocean interior at high latitudes (Stephens and Keeling, 2000).

Quantitative separation and attribution of the processes linking global ice volume, ocean temperature, and atmospheric CO_2 on millennial to orbital timescales are not currently available (e.g. Archer et al., 2000; Sigman et al., 2010; Gottschalk et al., 2019) and will not be attempted here. Rather, we make the simple assumption that the relationships between the LR04 benthic δ^{18}O stack and CO_2 can be extended beyond 800 ka and use generalised least-squares (GLS) regression modelling between benthic δ^{18}O and CO_2 to make a prediction of CO_2 spanning 800–1500 ka. The deliberately simple implicit assumption, and null hypothesis,

is that there is no change to the feedback processes linking benthic $\delta^{18}O$ and CO_2 before and after the MPT.

This approach differs from previous more complex model studies that have attempted to reconstruct CO_2 using the LR04 benthic $\delta^{18}O$ stack as an input variable (van de Wal et al., 2011; Stap et al., 2016; Berends et al., 2021a). Previous studies have used an inverse forward modelling approach, in which climate and ice sheet models of various complexities are used to capture physical relations between CO_2, global temperature, and ice volume. For example, in Berends et al. (2021a) the offset between modelled and observed benthic $\delta^{18}O$ is used to calculate a value for atmospheric CO_2 that is iterated back to the inverse model. The CO_2 record which minimises the difference between the modelled and observed benthic stack is then taken as an estimate of how atmospheric CO_2 may have evolved to force coupled climate, deep-ocean temperature, and land ice volume changes that reproduce the observed benthic $\delta^{18}O$ signal. The accuracy of the reconstructions in the inverse modelling approach depends on the ability of the climate and ice sheet models used to capture the correct climate dynamics across the MPT. Our GLS method is a simpler statistical approach, designed with the specific null hypothesis in mind, that does not attempt to simulate the physics linking benthic $\delta^{18}O$ signal, land ice volume, global temperature, and CO_2. A range of approaches to reconstructing CO_2 have been called for and are of value in the context of forthcoming continuous ice core records across the MPT from oldest ice projects currently underway in Antarctica (IPICS, 2020).

To test our null hypothesis in advance of the recovery of a continuous ice core, we compare our predicted CO_2 record to two sets of low-resolution ice core data that exist outside the current 800 kyr observed CO_2. These data come from direct CO_2 measurements from ancient "blue ice" from the Allan Hills in East Antarctica (hereafter referred to as BI-CO_2) from ca. 1 Ma (Higgins et al., 2015) and 1.5 Ma (Yan et al., 2022). We use the term blue ice to describe deep, ancient glacial ice that has been brought nearer to the surface of an ice sheet by ice flow. Blue ice is sampled by cutting trenches or shallow drilling of up to several hundred metres (e.g. Higgins et al., 2015). The vertical migration of blue ice is associated with high deformation, making the ice samples stratigraphically complex and hard to date (Higgins et al., 2015). As a result, blue ice records alone do not provide a continuous CO_2 record across the MPT. In the Discussion section, we also compare our predicted record to existing proxy CO_2 reconstructions from boron isotope analysis of benthic foraminifera in marine sediment records (Chalk, et al., 2017; Dyez et al., 2018; Guillermic et al., 2022), leaf wax $\delta^{13}C$ carbon isotope ratios (Yamamoto et al., 2022), and predictions from previous models of various complexities (van de Wal et al., 2011; Willeit et al., 2019; Berends et al., 2021a). We conclude with a discussion of the implications of our results and data comparisons for the understanding MPT dynamics.

2 Methods

We use a generalised least-squares (GLS) model with an autoregressive (AR) factor 1 to predict atmospheric CO_2 from the LR04 benthic $\delta^{18}O$ stack (Fig. 3a and b). We use GLS because the assumptions of ordinary least squares (OLS) are violated by the presence of autocorrelation and heteroskedasticity in the regression errors. We selected the AR(1) correlation factor as it yielded the lowest Akaike information criterion (AIC) value from a test of multiple correlation factors. The AR(1) process assumes and accounts for the dependence of error at a given point in time on the previous error term. In practise this makes the model assumptions more realistic and improves parameter estimation where, as in the climate system, observations are dependent on past values.

To obtain common time steps and resolution between the predictor (LR04 benthic $\delta^{18}O$ stack) and response (CO_2) variables, we re-grid the LR04 benthic stack and Bereiter et al. (2015) CO_2 data into time bins with a resolution of 3 kyr. The GLS regression model was then applied over the 0–800 kyr range of the predictor and response variables as follows:

$$CO_2 = -33.37 \times \delta^{18}O + 365.15,$$
$$\text{autoregressive (AR) factor:} 1. \tag{1}$$

Based on the regression model, the $\delta^{18}O$ values of the LR04 benthic stack from 800–1500 ka were used to predict CO_2 concentration over this range (hereafter referred to as PRED-CO_2). To gauge the GLS model stability we took a bootstrap approach, selecting a random 50 % subset of our data (with replacement) and re-running the model 1000 times to determine 95 % confidence intervals (CIs) for the predictions. While the GLS method itself addresses autocorrelation, the bootstrap method introduces variability such that each iteration of the model has different combinations of the original data points (including repeated ones); this variability helps assess the robustness and sensitivity of the model e.g. to variable data and dating uncertainty.

Uncertainties in the independent age scales of both the LR04 stack and the compiled CO_2 record are inherited by our GLS model and its predictions. The LR04 stack includes 57 globally distributed benthic $\delta^{18}O$ sediment core records. The age models for these cores are constructed by alignment of their $\delta^{18}O$ signals, followed by tuning of the stack to a simple ice model based on 21 June insolation at 65° N in a way which maintains relatively stable global mean sedimentation rates (Lisiecki and Raymo, 2005). The authors estimate uncertainty of 6 kyr from 1.5–1.0 Ma and 4 kyr from 1–0 Ma (Lisiecki and Raymo, 2005). The observed CO_2 composite ice core record for the past 800 kyr (Bereiter et al., 2015) uses six independent dating methods for various core locations both spatially across Antarctica and stratigraphically for different sections of the same core. The age uncertainty in the gas timescale has a median over the 0–800 ka interval of
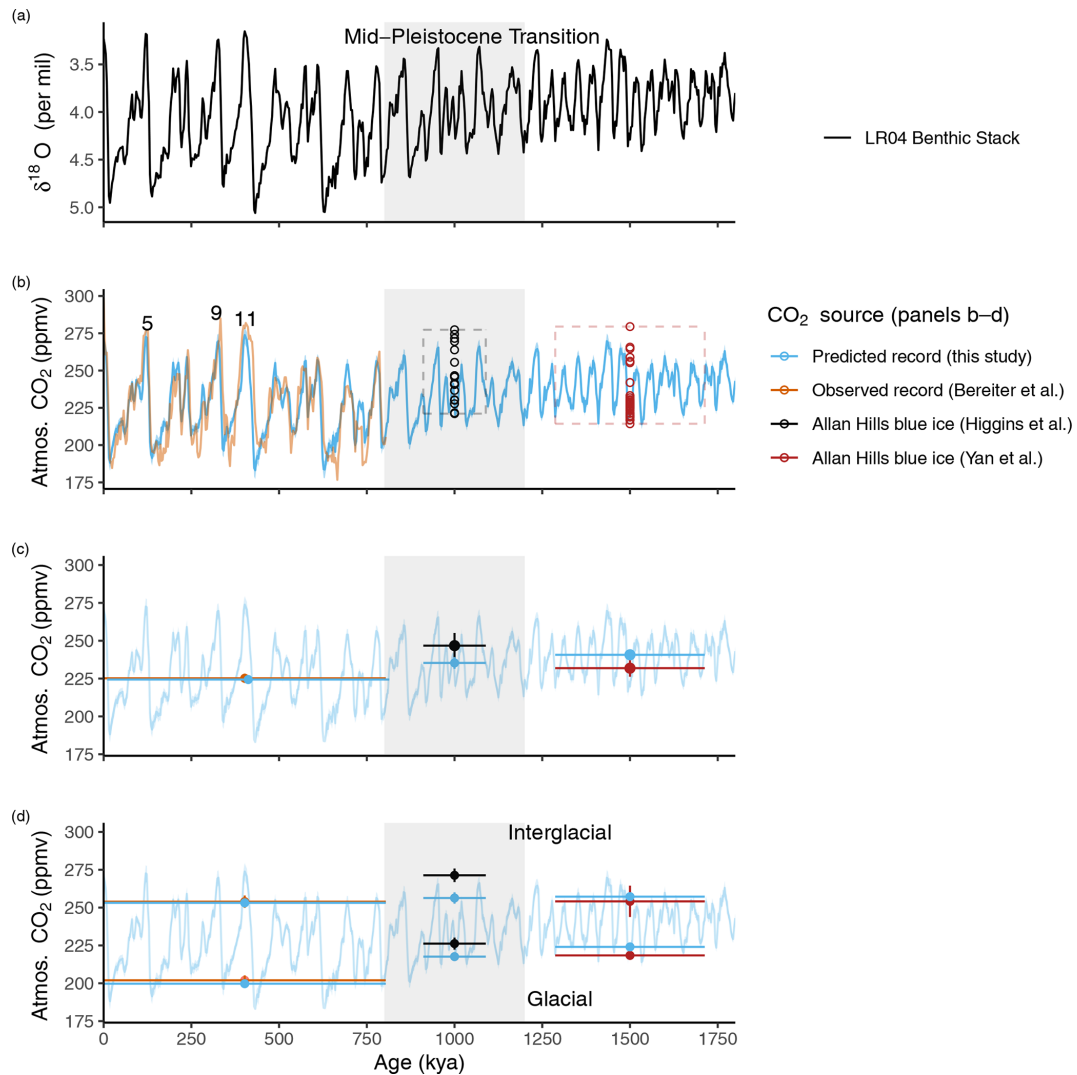
Figure 3. (a) The LR04 benthic stack of 57 globally distributed δ^{18}O records (Lisiecki and Raymo, 2005). **(b)** Comparison of our PRED-CO$_2$ (ppm) record to the current continuous composite record (0–800 ka) and to direct CO$_2$ measurements from Allan Hills blue ice cores (BI-CO$_2$) at ca. 1 Ma ($\pm$89 kyr) (Higgins et al., 2015) and ca. 1.5 Ma ($\pm$213 kyr) (Yan et al., 2022). Age uncertainty boundaries for the BI-CO$_2$ data are represented by dashed box boundaries. Marine isotope stages 5, 9, and 11 are numbered on the plot according to Lisiecki and Raymo (2005). Blue shading around PRED-CO$_2$ is the 95 % CI from bootstrap analysis. **(c)** Mean concentrations of the PRED-CO$_2$ and observed composite CO$_2$ records over the range of the observed composite record (offset for clarity) and the mean concentrations of the PRED-CO$_2$ and BI-CO$_2$ data at 1 Ma and again at 1.5 Ma averaged over the age uncertainty range of each BI-CO$_2$ dataset. **(d)** As for **(c)** but filtered by the upper and lower 25th and 75th percentiles to estimate glacial and interglacial periods.

2 kyr, but individual uncertainties can reach up to 5 kyr (Veres et al., 2013; Bazin et al., 2013). The relative age uncertainties between these input variables may diminish the regression or in some instances lead to spurious correlation. However, we expect any such effects are minor on the basis that our predictions show little sensitivity to the bootstrap analysis, with a median 2σ error of 5.8 ppm from 0 to 1.8 Ma (see Fig. 3b and c and the Discussion section).

3 Results

Figure 3b shows the time series of our LR04-benthic-δ^{18}O-stack-based GLS model predictions of atmospheric CO$_2$ (PRED-CO$_2$) over the past 800 kyr in comparison to the observed ice core CO$_2$ record from Bereiter et al. (2015). The correlation coefficient (R^2) between the predicted and observed records is 0.68 ($p \ll 0.01$). Our PRED-CO$_2$ record out to 1.8 Ma with shaded 95 % CIs from the bootstrap analysis is also shown, overlain with observed Allan Hills blue

ice CO_2 (BI-CO_2) datasets of age 1000 ± 89 ka (Higgins et al., 2015) and 1.5 Ma ± 213 kyr (Yan et al., 2022).

We evaluate the PRED-CO_2 record against the observed CO_2 data according to criteria of mean concentrations across the common intervals and mean concentrations in the glacial and interglacial subsets of the data. First is the mean CO_2 concentration over the common intervals (Fig. 3c). From 0–800 ka the mean concentrations in observed (Bereiter et al., 2015) and PRED-CO_2 data are in close agreement (225.2 ± 3.03 ppm versus the predicted 225.2 ± 2.5 ppm, respectively; uncertainties are 95 % confidence intervals, i.e. 1.96σ). In the 1000 ± 89 ka interval (i.e. averaged across the age uncertainty of the Higgins et al., 2015, blue ice data) the BI-CO_2 concentration is ~ 11 ppm higher than PRED-CO_2 (246.7 ± 8.4 ppm versus the predicted 235.3 ± 3.9 ppm); this difference is not significant at the 95 % confidence level. For the 1.5 Ma ± 213 kyr interval, the mean BI-CO_2 concentration is ~ 9 ppm lower than PRED-CO_2 (231.9 ± 5.6 ppm versus the predicted 240.7 ± 2.1 ppm), which is marginally significant at the 95 % level. Comparisons of mean levels across intervals spanning multiple glacial and interglacial cycles may be biased if (as is likely) the blue ice data are not sampling glacial and interglacial values with the same uniformity as a continuous record.

To address this, we define the glacial and interglacial thresholds of PRED-CO_2 to be the lower and upper 25th percentiles, respectively, of the LR04 $\delta^{18}O$ predictor variable (following Chalk et al., 2017). Filtering the observed (Bereiter et al., 2015) CO_2 record and our predicted CO_2 record according to these definitions, we find a very close match for glacial (202.0 ± 3.2 versus the predicted 199.7 ± 1.6 ppm) and interglacial intervals (253.9 ± 4.1 ppm versus the predicted 253.1 ± 2.3 ppm) over the past 800 kyr (see Fig. 3d for these comparisons). For blue ice (BI-CO_2) data, a corresponding LR04 isotope signal could not be confidently applied to the measured CO_2 concentration due to the uncertainties associated with blue ice dating; therefore, we defined the glacial and interglacial thresholds of blue ice data according to the top (interglacial) and bottom (glacial) 25th percentiles of actual CO_2. Applying this to the 1000 ± 89 ka interval finds that observed BI-CO_2 data are ~ 9 ppm higher than PRED-CO_2 during the glacial stages (226.2 ± 4.0 ppm versus the predicted 217.6 ± 2.3 ppm) and ~ 15 ppm higher than PRED-CO_2 during the interglacial stages (271.3 ± 4.5 versus the predicted 256.3 ± 3.8 ppm). These differences are significant with respect to the constrained uncertainties. During the 1.5 Ma ± 213 kyr interval, the mean BI-CO_2 concentration did not show any significant difference from PRED-CO_2 in interglacial stages (254.1 ± 10.3 versus the predicted 257.2 ± 1.7 ppm). During glacial stages there is a small 2.9 ppm difference between the upper estimate of BI-CO_2 and the lower estimate of PRED-CO_2 (218.4 ± 1.3 and 224 ± 1.4 ppm, respectively; see Fig. 3d). In our view these results, notwithstanding the 2.9 ppm difference at 1.5 Ma, do not give sufficient cause to reject the GLS model. Further-

more, the comparison indicates that PRED-CO_2 is not drifting systematically away from the existing observed BI-CO_2 data (Fig. 3d). The differences could of course represent a failing in the model, potential biases in the blue ice data, dating uncertainty, and/or other unconstrained uncertainties (see the Discussion section for blue ice caveats).

We now consider long-term trends in interglacial and (separately) glacial CO_2 levels across the past 1.8 Myr in PRED-CO_2 and in the existing ice core CO_2 data. For PRED-CO_2 there is no significant difference between CO_2 concentrations in the interglacial stages of the 1.5 Ma ± 213 ka, 1000 ± 89 ka, and 0–800 ka windows (Fig. 4d, blue bars). In the ice core observations, interglacial levels at 1.5 Ma in BI-CO_2 are also within the uncertainties of those in the 0–800 ka interval. Notably, the BI-CO_2 concentrations in the 1000 ± 89 ka interval appear elevated with respect to the 0–800 kyr and 1.5 Ma ± 213 ka intervals; however, this elevated (ca. 271 ppm) level is consistent with the observed interglacial CO_2 concentration during interglacials 5, 9, and 11 (Fig. 3b). Overall, there is no indication in the observed ice core CO_2 data or in PRED-CO_2 of a long-term trend in *interglacial* CO_2 levels across the past 1.8 Myr.

In comparison, there are significant declines in glacial CO_2 levels across the MPT in PRED-CO_2 and the observed ice core data. For PRED-CO_2, glacial CO_2 concentrations are not significantly different during the 1.5 Ma ± 213 ka and 1000 ± 89 ka windows. However, across the MPT, PRED-CO_2 glacial concentrations drop by ~ 18 ppm (Fig. 3d). This pattern is similar to the observed BI-CO_2 data, where glacial CO_2 levels show no decline between the 1.5 Ma ± 213 ka and 1000 ± 89 ka windows (indeed there is a marginal increase from 218.4 ± 1.3 to 226.2 ± 4.0 ppm, respectively), before falling by 24 ppm to the 0–800 kyr observed glacial mean of 202.0 ± 3.2 ppm (Fig. 3d). Glacial-stage drawdown of CO_2 across the MPT in the absence of interglacial drawdown is consistent with previous observations of boron-isotope-based CO_2 reconstructions (e.g. Chalk et al., 2017; Hönisch et al., 2009; see the Discussion section). In the following section we also compare PRED-CO_2 data to boron-isotope-based and other CO_2 proxy records covering the 0 to 1.8 Myr interval.

4 Discussion

Our objective with this paper was to generate the simplest reasonable model to predict CO_2 from the LR04 $\delta^{18}O$ benthic stack and to test the predictions against available observations. It is possible that the fit between observed and our predicted CO_2 data could be further improved using a non-linear approach. However, we refrain from a non-linear approach for several key reasons. First, a scatterplot of the LR04 $\delta^{18}O$ benthic stack versus observed ice core CO_2 over the past 800 kyr yields a Pearson's correlation coefficient (R) of -0.82 (Fig. 2), indicating that ~ 68 % of the variance
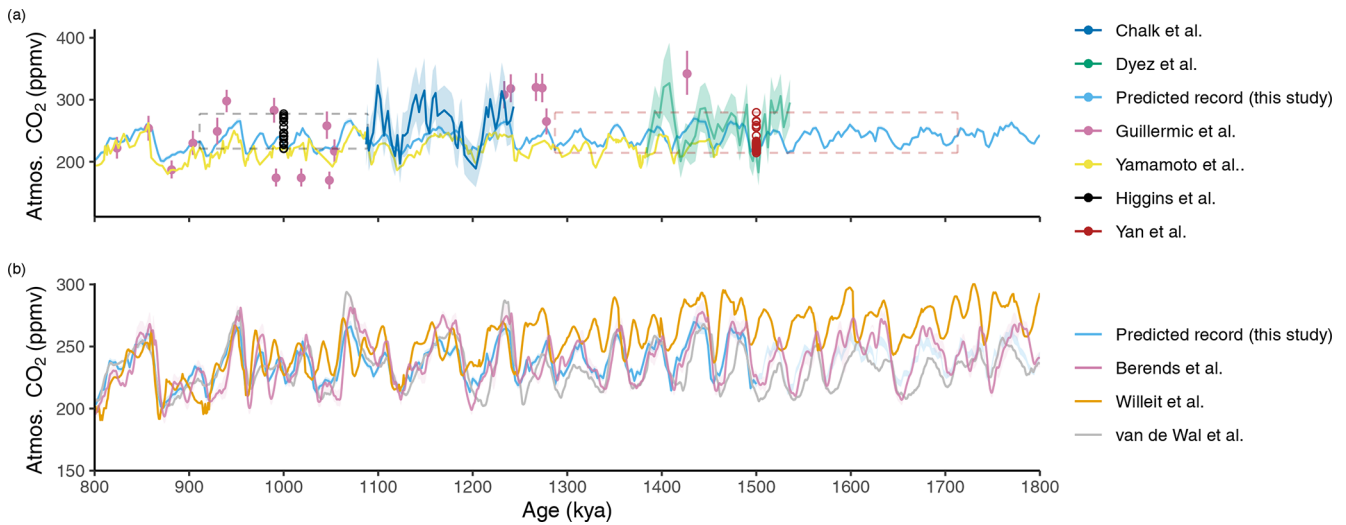
Figure 4. (a) Predicted CO_2 (this work) compared to observed proxy CO_2 estimates from a range of other sources: δ^{11}B-based pCO_2 reconstructions and measurements by Dyez et al. (2018), Guillermic et al. (2022), and Chalk et al. (2017); blue ice CO_2 measurements by Yan et al. (2019) and Higgins et al. (2015); and δ^{13}C leaf wax proxy reconstructions by Yamamoto et al. (2022). The dashed boxes indicate the dating uncertainty and range of the respective BI-CO_2 records. **(b)** Our predicted record compared to various model simulations: a regolith removal hypothesis simulation by Willeit et al. (2019) and inverse-model-based CO_2 reconstructions by van de Wal et al. (2011) and Berends et al. (2021a).

in observed CO_2 is shared with the benthic stack. This is similar to what was reported in ordinary linear least-squares regression ($R^2 = 0.70$) by Berends et al. (2021a). Importantly, there is no evidence in this scatterplot of departure from the linear relationship at high or low CO_2 or benthic δ^{18}O levels. Second, following the approach of Chalk et al. (2017) and interpreting the upper 25th percentile of CO_2 data as representing mean interglacial-stage CO_2 and the lower 25th percentile of CO_2 data as representing mean glacial-stage CO_2 levels, we see that our predicted interglacial mean value for the past 800 kyr (253.1 ± 2.3 ppm) closely overlaps with the observed interglacial mean value (253.9 ± 4.1 ppm), and similarly, the predicted glacial-stage mean (199.7 ± 1.7 ppm) closely overlaps with the observed glacial-stage mean (202.0 ± 3.2 ppm). Third, the predictions are remarkably insensitive to bootstrap analysis in which 50 % of the data are omitted with each iteration of the GLS model. Such insensitivity to the bootstrap analysis and accurate prediction of glacial and interglacial CO_2 values would be unlikely in the case of major non-linear dependencies between the LR04 predictor and CO_2 response variables. Fourth, non-linear approaches would risk generating an improved fit due to statistical artefacts that do not meaningfully relate to any dependence between benthic δ^{18}O and CO_2. Finally, the specific causes and sources and sinks involved in glacial to interglacial and millennial-scale CO_2 variations remain poorly constrained (e.g. Archer et al., 2000; Sigman et al., 2010; Gottschalk et al., 2019). Given this process uncertainty, the GLS model fits our criteria of the simplest reasonable model. Further, the use of benthic δ^{18}O to predict atmo-

spheric CO_2 has precedence; in response to the EPICA challenge (Wolff et al., 2004) Nicholas Shackleton predicted atmospheric CO_2 out to 800 kyr based on a number of benthic δ^{18}O records from the eastern Pacific (Wolff et al., 2005).

There are several caveats with blue ice data that may affect their use in evaluating our GLS model predictions. The blue ice data may have been subject to diffusional smoothing of CO_2 (e.g. Yan et al., 2019), which would act in the direction of elevating the (lower 25th percentile) assumed glacial concentrations above the glacial atmospheric values and reducing the (upper 25th percentile) assumed interglacial concentrations. There is also the potential for artificially elevated CO_2 concentrations in blue ice due to in situ respiration of CO_2 from microbial activity in detrital matter. Respiration effects are screened for by measurements of δ^{13}C of CO_2, but it is difficult to demonstrate that all samples are unaffected (Yan et al., 2019). These uncertainties support our argument that the GLS model predictions are not rejected by the available observed BI-CO_2 data.

We consider the BI-CO_2 data to provide the most reliable measurements of CO_2 concentration in the absence of a continuous ice core record across the MPT. However, further comparison of our CO_2 predictions can also be made against CO_2 proxy data from non-ice-core archives (Fig. 4a). We consider δ^{11}B-based atmospheric CO_2 reconstructions (Chalk et al., 2017; Dyez et al., 2018; Guillermic et al., 2022) and a recent atmospheric CO_2 reconstruction from δ^{13}C of leaf wax (Yamamoto et al., 2022). The continuous δ^{11}B-based reconstructions of Dyez et al. (2018) overlap PRED-CO_2 from ~ 1.38–1.5 Ma, while the Chalk et al. (2017) re-

construction overlaps PRED-CO_2 from 1.09–1.43 Ma. Discrete reconstructions from Guillermic et al. (2022) are distributed non-uniformly across the $\sim$ 800 to 1.5 Ma interval. For the two continuous δ^{11}B-based reconstructions (Chalk et al., 2017; Dyez et al., 2018) the glacial CO_2 levels appear to be consistent with the PRED-CO_2 record within their reported 30–60 ppm uncertainties. However, δ^{11}B-based interglacial stages in these reconstructions exceed those of the PRED-CO_2 record (Fig. 4a). The Guillermic et al. (2022) reconstructions suggest a larger range of CO_2 concentrations than the overlapping intervals of PRED-CO_2 and of the two continuous δ^{11}B-based reconstructions (Fig. 4a). The large range of the Guillermic et al. (2022) data and the high interglacial maxima in the Chalk et al. (2017) and Dyez et al. (2018) data all significantly exceed the range and interglacial maxima from the BI-CO_2 estimates. These discrepancies internally between different δ^{11}B-based CO_2 reconstructions and between the δ^{11}B-based reconstructions and the BI-CO_2 data may be due to uncertainties associated with the δ^{11}B proxy transfer function. The δ^{11}B-based CO_2 reconstructions are dependent on assumptions about multiple components of the carbonate system, including local marine carbon chemistry and the CO_2 saturation state in the past (Hönisch et al., 2009). Evidence that δ^{11}B-based reconstructions may overestimate interglacial-stage CO_2 is also seen in data from Chalk et al. (2017) spanning ca. 0–250 ka, where the δ^{11}B-based interglacial CO_2 levels exceed the continuous ice core CO_2 record by up to ca. 30 ppm.

By comparison, the δ^{13}C of leaf wax data (Yamamoto et al., 2022) have a similar glacial to interglacial range as PRED-CO_2 but a ca. 20 ppm lower mean concentration than our predictions (Fig. 4a). Hence, our PRED-CO_2 data fall lower than interglacial δ^{11}B-based interglacial levels but are higher than the δ^{13}C of leaf-wax-based estimates. The strong spread between these different proxies and the large associated uncertainty of the alternative marine and leaf wax proxy CO_2 reconstructions mean that we do not find cause from the existing CO_2 proxy data to reject our predictions or our associated null hypothesis.

We also compare our predictions to existing more complex model simulations (Fig. 4b), first against a transient simulation using an intermediate-complexity Earth system model (CLIMBER-2) by Willeit et al. (2019). This study suggests that a combination of gradual regolith removal and atmospheric CO_2 decline can explain the long-term climate variability over the past 3 Myr. The second comparison is against a longer-term reconstruction by van de Wal et al. (2011), which uses benthic δ^{18}O that utilises deep-sea benthic isotope records to reconstruct a continuous CO_2 record over the past 20 Myr. The third comparison is to a CO_2 reconstruction based on an inverse forward modelling approach forced by the LR04 benthic stack, in which the forward model is incrementally updated through interaction with general circulation model snapshots and the ANICE 3-D ice sheet–shelf model (Berends et al., 2021a). Our simple GLS

model demonstrates a similar long-term trend and timing of glacial–interglacial signals as well as an atmospheric CO_2 level that sits approximately mid-way between the van de Wal et al. (2011) and Willeit et al. (2019) models and is remarkably similar to the Berends et al. (2021a) reconstruction, despite their different approach. Notably the Berends et al. reconstruction shows greater glacial to interglacial amplitude in the CO_2 signal compared to our GLS model. The decreasing linear trend in CO_2 in Willeit et al. (2019), which is not seen in the other reconstructions, was directly prescribed in that study to induce Northern Hemisphere glaciation at 2.6 Myr ago.

A complete and critical test of our and other CO_2 predictions awaits the upcoming analysis of the continuous oldest ice core records. We now discuss some potential applications of the PRED-CO_2 record for hypothesis testing on the cause of the MPT.

PRED-CO_2 shows a long-term decline in glacial CO_2 across the MPT but no long-term decrease in interglacial CO_2. This pattern is consistent with the boron-isotope-based CO_2 reconstructions shown earlier, where it is often described as an increase in the interglacial to glacial CO_2 difference (e.g. Chalk et al., 2017; Hönisch et al., 2009). Chalk et al. (2017) conclude that the MPT was initiated by a change in ice sheet dynamics and that longer and higher-ice-volume post-MPT ice ages are sustained by carbon cycle feedbacks, in particular dust fertilisation of the Southern Ocean. The fact that our LR04-based prediction of CO_2 captures this same trend, with predicted glacial CO_2 fairly constant from 1.5 to ca. 1.0 Ma before declining from 1.0 to 0.6 Ma, reflects the fact that the LR04 benthic stack also features an increase in the interglacial to glacial benthic δ^{18}O difference across this same interval, which is dominated by the glacial-stage changes (Fig. 3a). Here, a comparison of PRED-CO_2 to a realised continuous oldest ice core record will be of value. The agreement or disagreement would provide information on the proportionality of the CO_2 coupling with ice volume; if there were a major new or non-linear process across the MPT that changed the nature of coupling between CO_2 and ice volume, the PRED-CO_2 and observed CO_2 records would be expected to diverge.

Another avenue to use the PRED-CO_2 record for hypothesis testing on the cause of the MPT concerns the phase locking hypothesis. The phase locking hypothesis is proposed to explain the absence of precession-related (23 kyr) periods in the LR04 benthic stack prior to the MPT (Fig. 1), despite the strong precession cycle in insolation (Raymo et al., 2006; Morée et al., 2021). The key concept is that prior to the MPT the Northern Hemisphere and Antarctic ice sheets were responsive (in ice volume) to insolation changes in the precession band, but because precession forcing is out of phase between the hemispheres, the ice volume changes were opposing between the hemispheres and therefore cancelled in the benthic stack. This cancellation of the precession signal left insolation forcing in the 41 kyr obliquity band to dom-

inate globally integrated ice volume changes expressed in the benthic stack. A transition from a smaller and more dynamic terrestrial-terminating Antarctic ice sheet to a larger and more stable marine-terminating ice sheet with cooling climate across the MPT (e.g. Elderfield et al., 2012) is then proposed to remove sensitivity of Antarctic ice volume to local precession forcing in favour of quasi-100 kyr ice volume changes that are in phase between the hemispheres (Raymo et al., 2006).

Recently presented data from Yan et al. (2022) lend some support to the phase locking hypothesis, specifically with evidence that pre-MPT Antarctic temperature (and by extension ice volume) is positively correlated with a local precession band insolation proxy based on the oxygen to nitrogen ratio of trapped air (Yan et al., 2022), whereas the correlation becomes negative in the blue ice and continuous ice core data in the post-MPT record. If Yan et al. (2022) are correct and the phase locking hypothesis holds, then an implication is that prior to the MPT, Antarctic climate, Antarctic ice volume, and by extension Southern Ocean climate conditions would fall out of phase with the LR04 benthic stack. To now extend the argument to potential impacts on CO_2 exchange, if the phase locking hypothesis holds, then prior to the MPT the Antarctic and Southern Ocean climate conditions and by extension the Southern Ocean mechanisms of CO_2 exchange described earlier would also be expected to fall out of phase with the benthic stack. Since our regression model assumes continuation of the in-phase relationship between the benthic stack and Antarctic and Southern Ocean climate conditions (as inherited from the post-MPT training data) we would expect to see major disagreement between our pre-MPT CO_2 predictions and a realised oldest ice continuous ice core CO_2 record.

5   Summary and conclusions

In this study we have used a simple generalised least-squares (GLS) model to predict atmospheric CO_2 from the LR04 benthic $\delta^{18}O$ stack for the period spanning the Mid-Pleistocene transition: 800–1800 kyr. Our CO_2 prediction is therefore based on the assumption that the physical processes linking CO_2, sea level, global ice volume, and ocean temperature over the past 800 kyr do not fundamentally change across the 800–1800 ka time period. The null hypothesis is deliberately simplistic on the basis that differences between our predictions and observed or proxy CO_2 records may be revealing of the physical processes involved in the Mid-Pleistocene Transition.

We made initial tests of the null hypothesis by comparing our predicted CO_2 record to existing discrete blue ice CO_2 records and other non-ice-core proxy CO_2 records from the 800–1800 kyr interval. Our predicted CO_2 concentrations do not show any systematic departure from observed blue ice CO_2 concentrations. The predictions are marginally lower

(during glacial *and* interglacial stages) than those observed in blue ice from 1000 ± 89 ka and marginally higher than observed in blue ice data from 1.5 Ma ± 213 kyr. Our predictions were generally lower than interglacial $\delta^{11}B$-based CO_2 reconstructions but higher than recent $\delta^{13}C$ of leaf-wax-based CO_2 reconstructions. Overall, we do not find clear evidence from the existing blue ice or proxy CO_2 data to reject our predictions or our associated null hypothesis. The definitive test of our and other CO_2 predictions therefore awaits the future analysis of the upcoming continuous oldest ice core records. The PRED-CO_2 record presented here should provide a useful comparison to forthcoming oldest ice core records and an opportunity for further constraints on the processes involved in the MPT.

Author contributions. Project design was created by JBP, TRV, and JRWM, and supervision was provided by TRV and JBP. Data analysis and figures were conducted by JRWM with input from all authors. Writing was led by JRMV and JBP. All authors contributed to and agreed on the final version of the manuscript.

Competing interests. The contact author has declared that none of the authors has any competing interests.

Disclaimer. This study, to the best of the authors' knowledge and belief, contains no material previously published or written by another person, except where due reference is made in the text of the study.

Publisher's note: Copernicus Publications remains neutral with regard to jurisdictional claims made in the text, published maps, institutional affiliations, or any other geographical representation in this paper. While Copernicus Publications makes every effort to include appropriate place names, the final responsibility lies with the authors.

Special issue statement. This article is part of the special issue "Oldest Ice: finding and interpreting climate proxies in ice older than 700 000 years (TC/CP/ESSD inter-journal SI)". It is not associated with a conference.

References

Archer, D., Winguth, A., Lea, D., and Mahowald, N.: What caused the glacial/interglacial atmospheric pCO_2 cycle?, Rev. Geophys., 38, 159–189, https://doi.org/10.1029/1999RG000066, 2000.

Bazin, L., Landais, A., Lemieux-Dudon, B., Toyé Mahamadou Kele, H., Veres, D., Parrenin, F., Martinerie, P., Ritz, C., Capron, E., Lipenkov, V., Loutre, M.-F., Raynaud, D., Vinther, B., Svensson, A., Rasmussen, S. O., Severi, M., Blunier, T., Leuenberger, M., Fischer, H., Masson-Delmotte, V., Chappellaz, J., and Wolff, E.: An optimized multi-proxy, multi-site Antarctic ice and gas orbital chronology (AICC2012): 120–800 ka, Clim. Past, 9, 1715–1731, https://doi.org/10.5194/cp-9-1715-2013, 2013.

Bereiter, B., Eggleston, S., Schmitt, J., Nehrbass-Ahles, C., Stocker, T. F., Fischer, H., Kipfstuhl, S., and Chappellaz, J.: Revision of the EPICA Dome C CO_2 record from 800 to 600 ky before present, Geophys. Res. Lett., 42, 542–549, https://doi.org/10.1002/2014gl061957, 2015.

Berends, C. J., de Boer, B., and van de Wal, R. S. W.: Reconstructing the evolution of ice sheets, sea level, and atmospheric CO_2 during the past 3.6 million years, Clim. Past, 17, 361–377, https://doi.org/10.5194/cp-17-361-2021, 2021a.

Berends, C. J., Köhler, P., Lourens, L. J., and van de Wal, R. S. W.: On the cause of the mid-Pleistocene transition, Rev. Geophys., 59, e2020RG000727, https://doi.org/10.1029/2020RG000727, 2021b.

Berger, A., Li, X. S., and Loutre, M. F.: Modelling northern hemisphere ice volume over the last 3 Ma, Quaternary Sci. Rev., 18, 1–11, https://doi.org/10.1016/S0277-3791(98)00033-X, 1999.

Broecker, W. S.: Glacial to interglacial changes in ocean chemistry, Prog. Oceanogr., 11, 151–197, https://doi.org/10.1016/0079-6611(82)90007-6, 1982.

Chalk, T., Hain, M., Foster, G., Rohling, E., Sexton, P., Badger, M., Cherry, S., Hasenfratz, A., Haug, G., Jaccard, S., Martínez-García, A., Pälike, H., Pancost, R., and Wilson, P.: Causes of ice age intensification across the Mid-Pleistocene Transition, P. Natl. Acad. Sci. USA, 114, 13114–13119, https://doi.org/10.1073/pnas.1702143114, 2017.

Clark, P. U. and Pollard, D.: Origin of the Middle Pleistocene Transition by ice sheet erosion of regolith, Paleoceanography, 13, 1–9, https://doi.org/10.1029/97pa02660, 1998.

Clark, P. U., Archer, D., Pollard, D., Blum, J. D., Rial, J. A., Brovkin, V., Mix, A. C., Pisias, N. G., and Roy, M.: The middle Pleistocene transition: characteristics, mechanisms, and implications for long-term changes in at-

mospheric pCO_2, Quaternary Sci. Rev., 25, 3150–3184, https://doi.org/10.1016/j.quascirev.2006.07.008, 2006.

Dyez, K. A., Hönisch, B., and Schmidt, G. A.: Early Pleistocene obliquity-scale pCO_2 variability at ~ 1.5 million years ago, Paleoceanogr. Paleoclimatol., 33, 1270–1291, https://doi.org/10.1029/2018PA003349, 2018.

Elderfield, H., Ferretti, P., Greaves, S., Crowhurst, S., McCave, N., and Piotrowski, A. M.: Evolution of Ocean Temperature and Ice Volume Through the Mid-Pleistocene Climate Transition, Science, 337, 704–709, https://doi.org/10.1126/science.1221294, 2012.

Gottschalk, J., Battaglia, G., Fischer, H., Frölicher, T. L., Jaccard, S. L., Jeltsch-Thömmes, A., Joos, F., Köhler, P., Meissner, K. J., Menviel, L., Nehrbass-Ahles, C., Schmitt, J., Schmittner, A., Skinner, L. C., and Stocker, T. G.: Mechanisms of millennial-scale atmospheric CO_2 change in numerical model simulations, Quaternary Sci. Rev., 220, 30–74, https://doi.org/10.1016/j.quascirev.2019.05.013, 2019.

Guillermic, M., Misra, S., Eagle, R., and Tripati, A.: Atmospheric CO_2 estimates for the Miocene to Pleistocene based on foraminiferal $\delta^{11}B$ at Ocean Drilling Program Sites 806 and 807 in the Western Equatorial Pacific, Clim. Past, 18, 183–207, https://doi.org/10.5194/cp-18-183-2022, 2022.

Hasenfratz, A. P., Jaccard, S. L., Martínez-García, A., Sigman, D. M., Hodell, D. A., Vance, D., Bernasconi, S. M., Kleiven, H. F., Haumann, F. A., and Haug, G. H.: The residence time of Southern Ocean surface waters and the 100 000 year ice age cycle, Science, 363, 1080, https://doi.org/10.1126/science.aat7067, 2019.

Higgins, J. A., Kurbatov, A. V., Spaulding, N. E., Brook, E., Introne, D. S., Chimiak, L. M., Yan, Y., Mayewski, P. A., and Bender, M. L.: Atmospheric composition 1 million years ago from blue ice in the Allan Hills, Antarctica, P. Natl. Acad. Sci. USA, 112, 6887, https://doi.org/10.1073/pnas.1420232112, 2015.

Hönisch, B., Hemming, N. G., Archer, D., Siddall, M., and McManus, J. F.: Atmospheric Carbon Dioxide Concentration Across the Mid-Pleistocene Transition, Science, 324, 1551, https://doi.org/10.1126/science.1171477, 2009.

Huybers, P. and Wunsch, C.: Obliquity pacing of the late Pleistocene glacial terminations, Nature, 434, 491–494, 2005.

International Partnerships in Ice Core Sciences (IPICS): The oldest ice core: A 1.5 million year record of climate and greenhouse gases from Antarctica [White paper], https://igbp-scor.pages.unibe.ch/sites/default/files/download/docs/working_groups/ipics/white-papers/ipics_oldaa_final.pdf (last access: 12 June 2023), 2020.

Jouzel, J., Masson-Delmotte, V., Cattani, O., Dreyfus, G., Falourd, S., Hoffmann, G., Minster, B., Nouet, J., Barnola, J. M., Chappellaz, J., Fischer, H., Gallet, J. C., Johnsen, S., Leuenberger, M., Loulergue, L., Luethi, D., Oerter, H., Parrenin, F., Raisbeck, G., Raynaud, D., Schilt, A., Schwander, J., Selmo, E., Souchez, R., Spahni, R., Stauffer, B., Steffensen, J. P., Stenni, B., Stocker, T. F., Tison, J. L., Werner, M., and Wolff, E. W.: Orbital and Millennial Antarctic Climate Variability over the Past 800 000 Years, Science, 317, 793, https://doi.org/10.1126/science.1141038, 2007.

Lisiecki, L. E. and Raymo, M. E.: A Pliocene-Pleistocene stack of 57 globally distributed benthic $\delta^{18}O$ records, Paleoceanography, 20, PA1003, https://doi.org/10.1029/2004pa001071, 2005.

Martínez-García, A., Sigman, D. M., Ren, H., Anderson, R. F., Straub, M., Hodell, D. A., Jaccard, S. L., Eglinton, T. I., and Haug, G. H.: Iron fertilization of the subarctic ocean during the last ice age, Science, 343, 1347–1350, https://doi.org/10.1126/science.1246848, 2014.

McClymont, E. L., Sosdian, S. M., and Rosell-Melé, A.: Pleistocene sea-surface temperature evolution: Early cooling, delayed glacial intensification, and implications for the mid-Pleistocene transition, Earth-Sci. Rev., 123, 173–193, https://doi.org/10.1016/j.earscirev.2013.04.006, 2013.

Millero, F. J.: Thermodynamics of the carbon dioxide system in the oceans, Geochim. Cosmochim. Ac., 59, 661–677, https://doi.org/10.1016/0016-7037(94)00354-O, 1995.

Morée, A. L., Sun, T., Bretones, A., Straume, E. O., Nisancioglu, K., and Gebbie, G.: Cancellation of the precessional cycle in $\delta^{18}O$ records during the Early Pleistocene, Geophys. Res. Lett., 48, e2020GL090035, https://doi.org/10.1029/2020GL090035, 2021.

Martin, J., Pedro, J., and Vance, T.: Predicting trends in atmospheric CO2 across the Mid-Pleistocene Transition using existing climate archives, Ver. 1, Australian Antarctic Data Centre [data set] and [code], https://doi.org/10.26179/7hkr-mz03, 2024.

Petit, J. R., Jouzel, J., Raynaud, D., Barkov, N. I., Barnola, J. M., Basile, I., Bender, M., Chappellaz, J., Davis, M., Delaygue, G., Delmotte, M., Kotlyakov, V. M., Legrand, M., Lipenkov, V. Y., Lorius, C., PÉpin, L., Ritz, C., Saltzman, E., and Stievenard, M.: Climate and atmospheric history of the past 420 000 years from the Vostok ice core, Antarctica, Nature, 399, 429–436, https://doi.org/10.1038/20859, 1999.

Raymo, M. E.: The timing of major climate terminations, Paleoceanography, 12, 577–585, https://doi.org/10.1029/97PA01169, 1997.

Raymo, M., Ruddiman, W., and Froelich, P.: Influence of Late Cenozoic mountain building on ocean geochemical cycles, Geology, 16, 649–653, https://doi.org/10.1130/0091-7613(1988)016<0649:IOLCMB>2.3.CO;2, 1988.

Raymo, M., Lisiecki, L., and Nisancioglu, K.: Plio-Pleistocene Ice Volume, Antarctic Climate, and the Global ^{18}O Record, Science, 313, 492–495, https://doi.org/10.1126/science.1123296, 2006.

Röthlisberger, R., Bigler, M., Wolff, E. W., Joos, F., Monnin, E., and Hutterli, M. A.: Ice core evidence for the extent of past atmospheric CO_2 change due to iron fertilisation, Geophys. Res. Lett., 31, L16207, https://doi.org/10.1029/2004GL020338, 2004.

Ruddiman, W. F., Raymo, M. E., Martinson, D. G., Clement, B. M., and Backman, J.: Pleistocene evolution: Northern hemisphere ice sheets and North Atlantic Ocean, Paleoceanography, 4, 353–412, https://doi.org/10.1029/PA004i004p00353, 1989.

Shackleton, N. J. and Pisias, N.G.: Atmospheric carbon dioxide, orbital forcing, and climate, in: The Carbon Cycle and Atmospheric CO_2: Natural Variations Archean to Present, edited by: Sundquist, E. T. and Broecker, W. S., American Geophysical Union, https://doi.org/10.1029/GM032p0303, 1985.

Shugi, H.: The older the ice, the better the science, Adv. Polar Sci., 23, 121–122, https://doi.org/10.13679/j.advps.2022.0004, 2022.

Sigman, D., Hain, M. P., and Haug, G. H.: The polar ocean and glacial cycles in atmospheric CO_2 concentration. Nature, 466, 47–55, https://doi.org/10.1038/nature09149, 2010.

Stap, L. B., de Boer, B., Ziegler, M., Bintanja, R., Lourens, L. J., and van de Wal, R. S. W.: CO_2 over the past 5 million years: Continuous simulation and new $\delta^{11}B$-based proxy data, Earth Planet. Sc. Lett., 439, 1–10, https://doi.org/10.1016/j.epsl.2016.01.022, 2016.

Stephens, B. B. and Keeling, R. F.: The influence of Antarctic sea ice on glacial–interglacial CO_2 variations, Nature, 404, 171–174, https://doi.org/10.1038/35004556, 2000.

Tzedakis, P. C., Crucifix, M., Mitsui, T., and Wolff, E. W.: A simple rule to determine which insolation cycles lead to interglacials, Nature, 542, 427–432, https://doi.org/10.1038/nature21364, 2017.

Ushie, H. and Matsumoto, K.: The role of shelf nutrients on glacial-interglacial CO_2: A negative feedback, Global Biogeochem. Cy., 26, GB2039, https://doi.org/10.1029/2011GB004147, 2012.

van de Wal, R. S. W., de Boer, B., Lourens, L. J., Köhler, P., and Bintanja, R.: Reconstruction of a continuous high-resolution CO_2 record over the past 20 million years, Clim. Past, 7, 1459–1469, https://doi.org/10.5194/cp-7-1459-2011, 2011.

Veres, D., Bazin, L., Landais, A., Toyé Mahamadou Kele, H., Lemieux-Dudon, B., Parrenin, F., Martinerie, P., Blayo, E., Blunier, T., Capron, E., Chappellaz, J., Rasmussen, S. O., Severi, M., Svensson, A., Vinther, B., and Wolff, E. W.: The Antarctic ice core chronology (AICC2012): an optimized multi-parameter and multi-site dating approach for the last 120 thousand years, Clim. Past, 9, 1733–1748, https://doi.org/10.5194/cp-9-1733-2013, 2013.

Willeit, M., Ganopolski, A., Calov, R., and Brovkin, V.: Mid-Pleistocene transition in glacial cycles explained by declining CO_2 and regolith removal, Sci. Adv., 5, eaav7337, https://doi.org/10.1126/sciadv.aav7337, 2019.

Wolff, E. W., Chappella, J., Fischer, H., Kull, C., Miller, H., Stocker, T. F., and Watson, A. J.: The EPICA challenge to the Earth system modeling community, EOS T. Am. Geophys. Un., 85, 363363, https://doi.org/10.1029/2004EO380003, 2004.

Wolff, E. W., Kull, C., Chappellaz, J., Fischer, H., Miller, H., Stocker, T. F., Watson, A. J., Flower, B., Joos, F., Köhler, P., Matsumoto, K., Monnin, E., Mudelsee, M., Paillard, D., and Shackleton, N.: Modeling past atmospheric CO_2: results of a challenge, EOS T. Am. Geophys. Un., 86, 341–345, https://doi.org/10.1029/2005EO380003, 2005.

Yamamoto, M., Clemens, S. C., Seki, O., Tsuchiya, Y., Huang, Y., O'ishi, R., and Abe-Ouchi, A.: Increased interglacial atmospheric CO_2 levels followed the mid-Pleistocene Transition, Nat. Geosci., 15, 307–313, https://doi.org/10.1038/s41561-022-00918-1, 2022.

Yan, Y., Benderm M. L., Brook, E. J., Clifford, H. M., Kemeny, P. C., Kurbatov, A. V., Mackay, S., Mayewski, P. A., Ng, J., Severinghaus J. P., and Higgins, J. A.: Two-million-year-old snapshots of atmospheric gases from Antarctic ice, Nature, 574, 663–666, https://doi.org/10.1038/s41586-019-1692-3, 2019.

Yan, Y., Kurbatov, A. V., Mayewski, P. A., Shackleton, S., and Higgins, J. A.: Early Pleistocene East Antarctic temperature in phase with local insolation, Nat. Geosci., 16, 50–55, https://doi.org/10.1038/s41561-022-01095-x, 2022.